Proceedings of the 1997 IEEE
International Conference on Robotics and Automation
Albuquerque, New Mexico - April 1997

Slip Modelling and Aided Inertial Navigation of an LHD

S. Scheding, G. Dissanayake, E. Nebot and H. Durrant-Whyte
Department of Mechanical Engineering
The University of Sydney, NSW. 2006, Australia
e-mail: scheding/dissa/nebot/hugh @tiny.me.su.OZ.AU

Abstract

This paper describes the theoretical development and experimental evaluation of a guidance system for an autonomous Load, Haul and Dump truck (LHD) for use in underground mining. The particular contributions of this paper are in designing the navigation system to be able to cope with vehicle slip in rough uneven terrain using information from an Inertial Navigation System (INS) and a bearing only laser. Results are presented using data obtained during field trials.

1 Introduction

The LHD (see Figure 1) is the workhorse of underground mining. A typical use for the LHD is in moving ore from the rock face to a centralised dumping point. There is a strong case for automation of these trucks, for reasons of both safety and productivity. The safety issue has been addressed with several working implementations of teleoperated systems, including the well publicised Canadian system [1][2]. Teleoperation, however, offers little to increase productivity, as these systems tend to run at speeds similar to, or slower than, conventional manned systems, thus keeping existing (or lesser) productivity levels, with the additional overhead of the infrastructure required to teleoperate. The next step to increasing productivity whilst maintaining safety is therefore to completely automate the LHD, using as little infrastructure as possible.

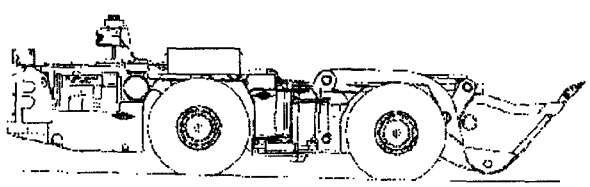

Figure 1: A Typical LHD

Several autonomous LHD systems have been trialled, including [3] which uses a retroreflective stripe on the tunnel roof (back) detected by cameras to guide the vehicle. In [4], a system is proposed that uses ultrasonic sensors to follow the walls of a tunnel. Although these systems work, their scope is limited. The reflective stripe system requires relatively major levels of infrastructure, which must be changed whenever a new path is required for the vehicle, whilst the ultrasonic approach suffers from lack of an Earth-fixed coordinate system, which is necessary for any planning operations, particularly traffic management.

A more robust approach is presented in [5], where information from various sensors is fused via an Extended Kalman Filter, to provide an estimate of position and orientation. This approach, however, suffers from under utilisation of data. The vehicle model presented uses heading provided from a gyro, coupled with encoder derived velocity information. Information about articulation angle (described later) of the vehicle is simply ignored.

This paper discusses the development of a navigation system for an autonomous underground LHD mining vehicle. The key issues addressed in this paper are the explicit modelling of slip parameters as the vehicle manouevers over rough terrain, and the use of inertial measurements to estimate these parameters. Data from extensive field trials has shown that the levels of slip induced by the turning vehicle are non-negligible and cannot be ignored. As the slip experienced by the vehicle is difficult to measure directly, the slip parameters must be estimated using a statistical filter by processing information taken from on-board sensors. Because of the high levels of slip, it is essential to use information from sensors sensing relative to an inertial frame of reference, in this case an Inertial Navigation System (INS). A rotating laser scanner is also used to provide periodic updates relative to fixed known landmarks.

This paper is organised as follows. The Vehicle model section details the evolution of, and reasons for a vehicle model which explicitly incorporates slip. This section also details the way the various errors in the system are modelled and the way the sensors themselves are modelled. The Implementation section summarises how the continuous time models may be discretised for realtime implementation on a digital computer. A results section follows which discusses in detail an example using real data obtained

0-7803-3612-7-4/97 $5.00

underground on an LHD, and concluding remarks are made in the final section.

2 Vehicle Model

The key to designing navigation systems for autonomous vehicles is the model which describes how the vehicles position and other key vehicle parameters evolve through time. The model is essential to make good use of sensor data and for describing how unobserved vehicle parameters affect vehicle motion. This model usually consists of two parts, the vehicle model itself, and a model which describes how errors in the vehicle model propagate in time.

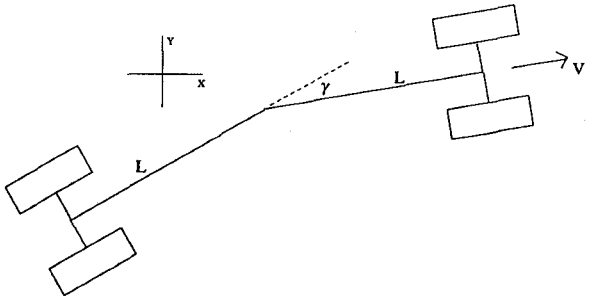

Figure 2: LHD Kinematic Geometry

The LHD is an articulated vehicle, which means that the vehicle has a front and rear body which can rotate relative to each other. The front and rear wheel sets are fixed to remain parallel with the body of the vehicle, and steering is achieved by driving the articulation joint located midway between the front and rear axles. Figure 2 shows the geometry of a typical LHD.

2.1 The No-Slip Model

The kinematic model of the vehicle derived from rigid body and rolling motion constraints is given by;

$$\begin{aligned} \dot{x}(t) &= V\cos(\phi) \\ \dot{y}(t) &= V\sin(\phi) \\ \dot{\phi}(t) &= \frac{V\tan(\frac{\gamma}{2})}{L} \end{aligned} \tag{1}$$

where x and y denote the position of the vehicle relative to some fixed global frame of reference. ϕ is the orientation of the vehicle with respect to the x axis, while V represents the linear velocity of an imaginary front wheel located midway between the real front wheels. γ is defined as the articulation angle of the vehicle, and L is the half-length of the vehicle, the distance between the front set of wheels and the articulation joint.

The derivation is omitted here, but the result concurs with [4].

However, for the particular LHD used in the experimental work, an Atlas-Copco Wagner ST-7, the drivetrain delivers equal power to both the front and rear wheel sets through the transmission. This guarantees that wheel slip must occur when the rate of change of the articulation angle is non-zero. This means that the constraint of zero velocity in the direction of the axles (rolling motion constraint) is not valid, and in fact this model greatly overestimates the rate of change of orientation $\dot{\phi}$. A new kinematic model that explicitly models this slip is therefore developed as follows.

2.2 Accounting for Slip

To take into account that the vehicle will slip during motion, two slip variables α and β are introduced. These variables are chosen to represent the slip angles of the vehicle, that is, the angle between the kinematically indicated velocity (perpendicular to the axles) and the true velocity. The variation between true and kinematic velocities is by definition entirely dependent on the slip.

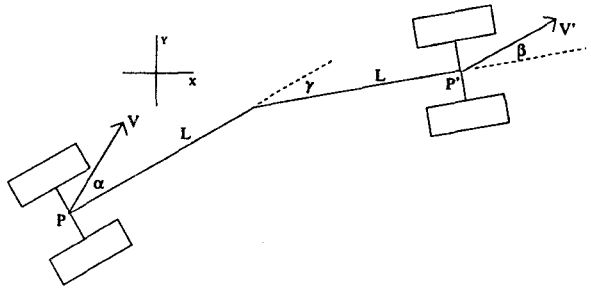

Figure 3: LHD Kinematic Geometry - Including Slip Angles

Consider the velocity of the point P in the rear body, and the velocity at a symmetric point P' in the front body as shown in Figure 3. Generally, the prime will indicate quantities related to the front of the vehicle, whilst no prime indicates quantities related to the rear.

By obtaining the velocity of P' in the direction perpendicular to V' and equating this to zero, we obtain the following relation;

$$\begin{aligned} V\sin(\alpha-\beta-\gamma)+L\cos(\beta+\gamma)\dot{\phi} \\ + L\cos(\beta)(\dot{\phi}+\dot{\gamma}) = 0 \end{aligned}$$

which may be solved for $\dot{\phi}$ to yield

$$\dot{\phi} = \frac{(\omega R\sin(\beta-\alpha+\gamma) - \dot{\gamma}L\cos(\beta))}{L(\cos(\beta)+\cos(\beta+\gamma))}$$

If the velocity V of P is now set to equal ωR , the wheels angular velocity multiplied by the nominal wheel radius, and resolved into x and y, the following kinematic equations for the motion of point P are

obtained;

$$\begin{aligned}\dot{x} &= \omega R\cos(\alpha+\phi)\\ \dot{y} &= \omega R\sin(\alpha+\phi)\\ \dot{\phi} &= \frac{(\omega R\sin(\beta-\alpha+\gamma)-\dot{\gamma}L\cos(\beta))}{L(\cos(\beta)+\cos(\beta+\gamma))}\end{aligned} \quad (2)$$

It can be seen that the vehicle moves in the direction given by the slip angle, ie the vehicle heads in the direction $\alpha+\phi$, whilst the rate of change of orientation is dependant on the slip angles, the articulation angle, and the rate of change of articulation angle.

2.3 The Importance of Slip

Comparing Equation 2 to Equation 1, it can be seen that the models are significantly different, particularly for the term $\dot{\phi}$. The simple model described by Equation 1 greatly overestimates the turning rate of the vehicle, causing the navigation system to continuously fight to correct the modelling error. Equation 2 is far more accurate if the slip angles are known. This is where the EKF plays an important part, because states that are not directly observable, such as the slip parameters, may be estimated and used to improve the model of the vehicle.

As the vehicle drives both the front and rear wheel sets at the same angular velocities, insight into why the vehicle does indeed slip may be gained by examining the different expressions for V and V'. The equation governing V' is;

$$V' = \frac{V(\cos(\alpha-\gamma)+\cos(\alpha))-L\dot{\gamma}\sin(\gamma)}{\cos(\beta)+\cos(\beta+\gamma)}$$

When the slip angles α and β are zero (ie no slip is present), we obtain the following expression for the velocity of the front wheel.

$$V' = V - L\dot{\gamma}\tan(\frac{\gamma}{2})$$

It is clear from this that the only conditions under which the front and rear velocities are equal (under no-slip assumptions) is when the articulation angle γ is constant or zero. Therefore wheel slip must be present. Experimental data shows that the rate of change of articulation angle $\dot{\gamma}$ can be quite high, and may cause the vehicles tyres to scrub the ground. Human operators tend to use this effect to their advantage.

2.4 The Error Model

When the model addressed in Equation 2 is considered, it can be seen that the primary sources of error are due to the time varying parameters ω, γ, $\dot{\gamma}$, α and β, as errors in these parameters propagate directly through to the states. The variables ω, γ and $\dot{\gamma}$ represent well known control inputs and thus do not need to be estimated. The slip parameters α and β, however, are not directly measured, and therefore cannot be treated in the same way as the control inputs. It is interesting to note that the effective wheel radius of the vehicle can also be considered to be time varying and takes into account factors such as loading and tyre wear. The wear on a typical LHD tyre can be as much as $15-20cm$ in radius and will therefore introduce a bias to the system over the operating lifetime of the tyres if a constant wheel radius is assumed. The concept of estimating wheel radius was introduced in [6], and is extremely beneficial to this application. Therefore, the states to be estimated should not only include position and orientation, but also the slip angles and wheel radius.

It is salient at this point to describe how the error in each of the parameters may be modelled, as it is important to know how the errors propagate through time. The errors in control input are modelled as simple additive noise $\delta\omega(t)$, $\delta\gamma(t)$ and $\delta\dot{\gamma}(t)$ about their respective means $\bar{\omega}(t)$, $\bar{\gamma}(t)$ and $\bar{\dot{\gamma}}(t)$ at time t such that

$$\begin{aligned}\omega(t) &= \bar{\omega}(t)+\delta\omega(t)\\ \gamma(t) &= \bar{\gamma}(t)+\delta\gamma(t)\\ \dot{\gamma}(t) &= \bar{\dot{\gamma}}(t)+\delta\dot{\gamma}(t)\end{aligned}$$

The errors in R, α and β, however, are extremely difficult to model accurately as they tend to involve a combination of other parameters, as they are caused fundamentally by the vehicle dynamics. For example, the error in slip angle will change with respect to vehicle speed, mass, tyre-terrain interaction and articulation angle in a highly non-linear way. A compromise which has been found to work well is to model the errors in these parameters as random walks (or brownian motion), such that the error in each of the parameters is the integral of white noise as follows,

$$\begin{aligned}\dot{R}(t) &= \delta R(t)\\ \dot{\alpha}(t) &= \delta\alpha(t)\\ \dot{\beta}(t) &= \delta\beta(t)\end{aligned}$$

The noise sources $\delta\omega(t)$, $\delta\gamma(t)$, $\delta\dot{\gamma}(t)$, $\delta R(t)$, $\delta\alpha(t)$ and $\delta\beta(t)$ are assumed zero-mean, uncorrelated gaussian sequences with variance σ_ω^2, σ_γ^2, $\sigma_{\dot{\gamma}}^2$, σ_R^2, σ_α^2 and σ_β^2 respectively.

The continuous time vehicle model shown in Equation 2 may now be rewritten at time t, adding the additional states to be estimated as;

$$
\begin{aligned}
\dot{x}(t) &= \omega(t)R(t)\cos(\alpha(t)+\phi(t)) \\
\dot{y}(t) &= \omega(t)R(t)\sin(\alpha(t)+\phi(t)) \\
\dot{\phi}(t) &= \frac{\omega(t)R(t)\sin(\beta(t)-\alpha(t)+\gamma(t))}{L(\cos(\beta(t))+\cos(\beta(t)+\gamma(t)))} \\
&\quad -\frac{\dot{\gamma}(t)L\cos(\beta(t)))}{L(\cos(\beta(t))+\cos(\beta(t)+\gamma(t))} \\
\dot{R}(t) &= \delta R(t) \\
\dot{\alpha}(t) &= \delta\alpha(t) \\
\dot{\beta}(t) &= \delta\beta(t) \qquad (3)
\end{aligned}
$$

2.5 Observation Model

The vehicle has a laser sensor (see Figure 4) which is capable of detecting the angle to a number of fixed beacons $\mathbf{B}_i = [X_i, Y_i]^T, i = 1, \ldots, N$. This sensor, although in practise very good, only allows the state to be updated periodically, or at a low frequency.

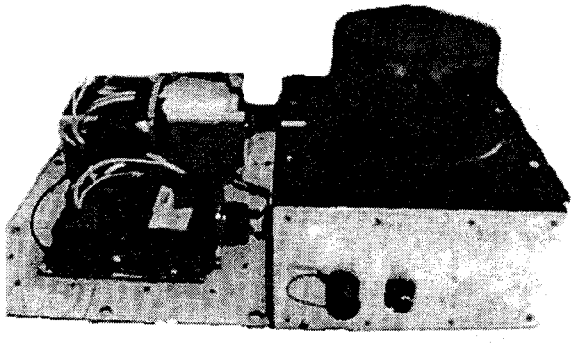

Figure 4: The INS and Laser used in the field trials

To augment the system with gyro information, information from the three gyros is first converted to a single rotation about the vehicles z axis, then fused in the filter to provide a better estimate of state. Gyros are well known to drift with time, a low frequency error which is fed straight through to the estimate if the gyro drift is not compensated for. By using a shaping filter however, the low frequency errors in the gyro information may be modelled, and are thus rejected by the filter.

The errors in the gyro are adequately modelled as Brownian motion, the integral of white noise. The shaping state for brownian motion is given by

$$\dot{x}_{sf}(t) = \mathbf{w}_{sf}(t) \qquad (4)$$

Where $\mathbf{w}_{sf}(t)$ represents a gaussian sequence with variance σ^2_{sf}. The shaping state must now be used to augment the state vector as follows.

$$\mathbf{x}(t) = [x(t), y(t), \phi(t), R(t), \alpha(t), \beta(t), x_{sf}(t)]^T \qquad (5)$$

The observations which the sensors will make are assumed to be of the form

$$\mathbf{z}(t) = \mathbf{h}(\mathbf{x}(t)) + \mathbf{w}(t) \qquad (6)$$

where $\mathbf{z}(t)$ represents the observation vector, $\mathbf{h}(\cdot)$ is the non-linear matrix mapping observations to states and $\mathbf{w}(t)$ is additive sensor noise, assumed gaussian and with zero mean.

The bearing to a beacon may be given by $\arctan(\frac{Y_i - y(t)}{X_i - x(t)})$, however the vehicle is oriented in the direction ϕ, so for this system, the measurement equation for each beacon detected by the laser is given by the non-linear model,

$$\mathbf{z}^i_\theta(t) = \left[\arctan(\frac{Y_i - y(t)}{X_i - x(t)}) - \phi(t)\right] + [w^i_\theta(t)] \qquad (7)$$

and the measurement equation for the gyro is given by the linear model,

$$\mathbf{z}_{gyro}(t) = [\phi(t) + x_{sf}(t)] + [w_{gyro}(t)] \qquad (8)$$

which is an observation of the orientation plus the shaping state which represents gyro drift.

3 Implementing the Navigation System

To implement a filter based on a continuous time model, the model must be discretised. The control signals ω and γ and the sensor observations are sampled at regular discrete intervals. The sample interval ΔT, is synchronous and small enough to capture manouvers occuring in the operating frequency range. The control inputs ω, γ and $\dot{\gamma}$ are assumed approximately constant over this interval.

For the EKF, the non-linear state transition equation (the discrete time equivalent of the process model) is given by,

$$\mathbf{x}(k+1) = \mathbf{f}(\mathbf{x}(k), \mathbf{u}(k), k) + \mathbf{v}(k)$$

which may be readily obtained from Equation 3 using a first order Euler approximation as,

$$
\begin{aligned}
x(k+1) &= x(k) + \Delta T\omega(k)R(k)\cos(\alpha(k)+\phi(k)) \\
y(k+1) &= y(k) + \Delta T\omega(k)R(k)\sin(\alpha(k)+\phi(k)) \\
\phi(k+1) &= \phi(k) \\
&\quad + \frac{\Delta T\omega(k)R(k)\sin(\beta(k)-\alpha(k)+\gamma(k))}{L(\cos(\beta(k))+\cos(\beta(k)+\gamma(k)))} \\
&\quad - \frac{\Delta T\dot{\gamma}(k)L\cos(\beta(k))}{L(\cos(\beta(k))+\cos(\beta(k)+\gamma(k))} \\
R(k+1) &= R(k) + \Delta T\delta R(k) \\
\alpha(k+1) &= \alpha(k) + \Delta T\delta\alpha(k) \\
\beta(k+1) &= \beta(k) + \Delta T\delta\beta(k) \\
x_{sf}(k+1) &= x_{sf}(k) + \Delta T\delta\mathbf{w}_{sf}(k)
\end{aligned}
$$

Similarly, the non-linear sensor model is assumed of the form

$$\mathbf{z}(k) = \mathbf{h}(\mathbf{x}(k)) + \mathbf{w}(k)$$

which in this case may be obtained directly from Equations 7 and 8.

The EKF algorithm consists of a prediction-update cycle where prediction is performed when either no sensor information is available or to predict the state at the next discrete time-step. An update occurs when sensor information is available to improve the systems estimate of state. For a full derivation of an EKF for a system of this type, refer to [6].

4 Results

The results presented here were obtained using data from field trials on an LHD in an underground mine in Queensland, Australia. An LHD was retro-fitted with a potentiometer mounted on the articulation joint to provide angular information. An inductive sensor normally used for condition monitoring purposes was used to sense the angular velocity of the drive train. The laser scanner and INS were mounted on the rear of the vehicle. The sensor positions were measured accurately so that coordinate transformations could be reliably achieved. The experimental setup is described further in [7].

The trials themselves utilised a section of tunnel approximately one hundred and fifty metres long, populated with retroreflective strips used as beacons for the laser scanner. The strips were surveyed to provide their positions in the tunnel. The data from all sensors on board the vehicle was logged and time-stamped during the trials, and post processed to provide the results seen here.

Figure 5 shows the tracked path of the LHD during a greater than right angle turning manoeuvre. The maximum standard deviation, or error bound in position during this manoeuvre (as estimated by the EKF) was approximately eight centimetres as can be seen in Figure 6. Figures 8, 9 and 10 show the estimated wheel radius and the slip angles α and β respectively. These may be compared to Figure 7 which shows the variation in articulation angle over time. As can be seen from these graphs, the estimated slip is highly correlated with the articulation angle, verifying the intuitive assumption that the vehicle will slip more while cornering. This is of particular importance in underground mining where a majority of the tunnel corners are tight right angled bends. In this example, the forward slip angle β approaches six degrees during the corner, while the rear slip angle α exceeds twenty degrees. It is also interesting to note that the estimated wheel radius R decreases by approximately $0.1m$ during the manoeuvre. The reason for this effect is clear when we consider that the vehicles forward velocity is given by $V = \omega R$. Any change in the forward velocity of the vehicle (due to forward slip) is estimated as a change in wheel radius by the EKF. The slip angles account for the across axis, or transverse, slip.

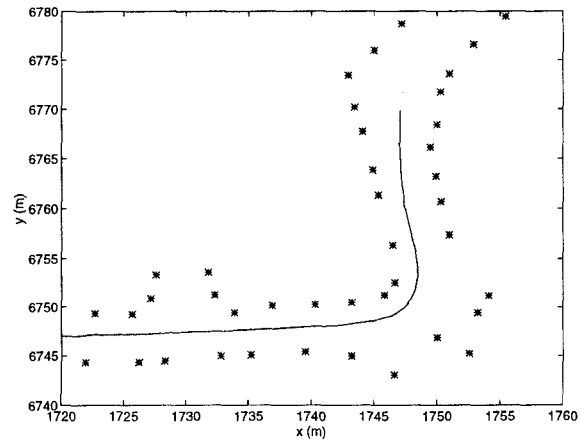

Figure 5: Estimated LHD Path - stars represent retroreflective markers

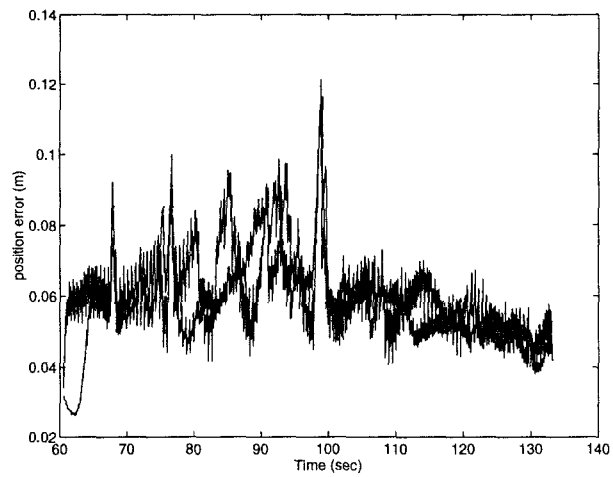

Figure 6: Position standard deviation during run (x and y)

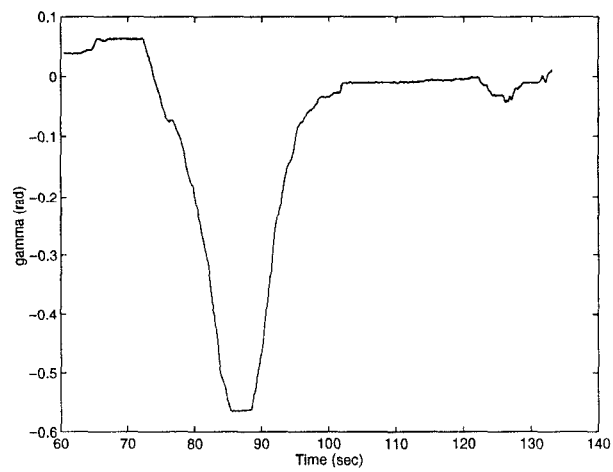

Figure 7: Articulation Angle Gamma

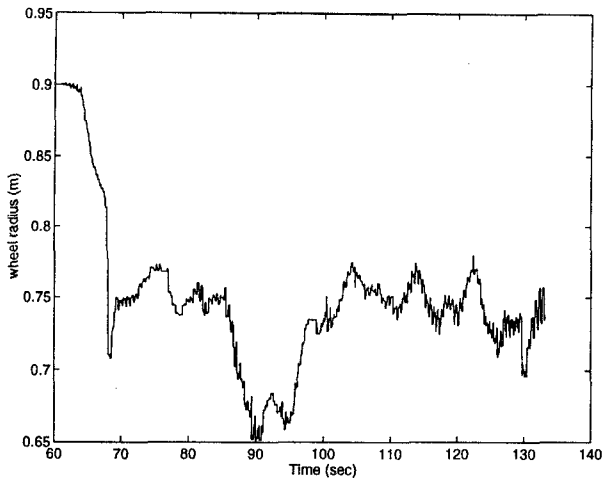

Figure 8: Estimated Wheel Radius

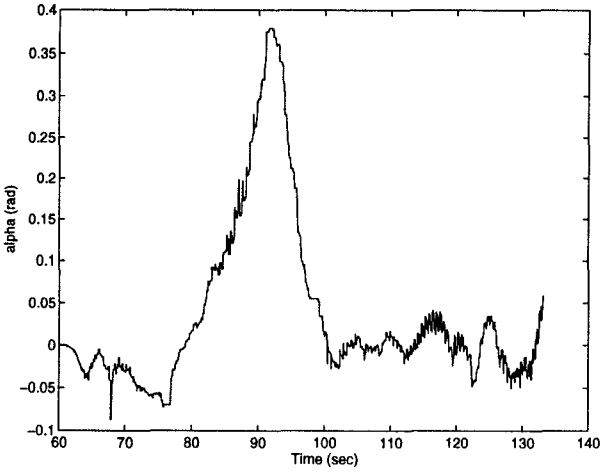

Figure 9: Estimated Slip Angle Alpha

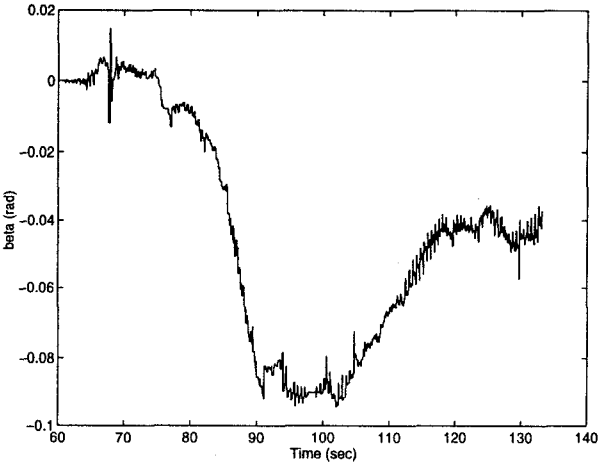

Figure 10: Estimated Slip Angle Beta

5 Conclusions

In this paper, an LHD vehicle model which explicitly incorporates slip was presented. A navigation system was described in which observations from a laser sensor and from an INS unit are incorporated to aid the estimation of the slip angles. The results clearly show that the amounts of slip experienced by the vehicle are non-negligible particularly during cornering. In this case, the no-slip model simply fails. The benefits of this approach are in making the navigation systems for large heavy industrial machinery much more reliable and robust in harsh uneven terrain. Future research in this area will include the addition of a full INS unit, including accelerometers to aid the navigation system, and research into the use of redundant navigation packages to detect system faults. The theory described in this paper will be extended for use in outdoor applications.

References

1. F. Labonte and P. Cohen, "Perceptual Aspects of Mining Equipment Teleoperation," in *Proceedings of the 6th Canadian Symposium on Mining Automation*, 1994.

2. F. Labonte, J. Giraud, and V. Polotski, "Telerobotics Issues in the Operation of a LHD Vehicle," in *Proceedings of the Third Canadian Conference on Computer Applications in the Mineral Industry*, 1995.

3. G. Baiden, "Multiple LHD Teleoperation and Guidance at Inco Limited," in *Proceedings of the International Mining Congress*, 1993.

4. J. Steele, C. Ganesh, and A. Kleve, "Control and Scale Model Simulation of Sensor-Guided LHD Mining Machines," *IEEE Transactions on Industry Applications*, vol. 29, pp. 1232–1238, 1993.

5. H. Makela, H. Lehtinen, K. Rintanen, and K. Koskinen, "Navigation System for LHD Machines," *Intelligent Autonomous Vehicles*, pp. 314–319, 1995.

6. H. F. Durrant-Whyte, "An Autonomous Guided Vehicle for Cargo Handling Applications," *International Journal of Robotics Research*, vol. 15, 1996.

7. S. Scheding, E. Nebot, and H. F. Durrant-Whyte, "Experiments in Underground Guidance," in *IEEE Conference on Robotics and Automation*, 1997.